Stagno *et al. Progress in Earth and Planetary Science* (2021) 8:27
https://doi.org/10.1186/s40645-021-00421-y

Progress in Earth and Planetary Science

RESEARCH ARTICLE Open Access

Can quasicrystals survive in planetary collisions?

Vincenzo Stagno[1], Luca Bindi[2*], Sota Takagi[3] and Atsushi Kyono[4]

Abstract

We investigated the compressional behavior of i-AlCuFe quasicrystal using diamond anvil cell under quasi-hydrostatic conditions by in situ angle-dispersive X-ray powder diffraction measurements (in both compression and decompression) up to 76 GPa at ambient temperature using neon as pressure medium. These data were compared with those collected up to 104 GPa using KCl as pressure medium available in literature. In general, both sets of data indicate that individual *d*-spacing shows a continuous decrease with pressure with no drastic changes associated to structural phase transformations or amorphization. The d/d_0, where d_0 is the *d*-spacing at ambient pressure, showed a general isotropic compression behavior. The zero-pressure bulk modulus and its pressure derivative were calculated fitting the volume data to both the Murnaghan- and Birch-Murnaghan equation of state models. Results from this study extend our knowledge on the stability of icosahedrite at very high pressure and reinforce the evidence that natural quasicrystals formed during a shock event in asteroidal collisions and survived for eons in the history of the Solar System.

Keywords: Icosahedrite, Quasicrystal, CV3 chondrite, Khatyrkite, In situ angle-dispersive X-ray diffraction

1 Introduction

Textural and chemical studies of shocked veins and mineral assemblages observed in meteorites over the last decades have been widely interpreted in light of dynamic (e.g., shock experiments) and static (e.g., multi anvil and diamond anvil cell experiments) compression investigations of diverse minerals and their stability at high (H) pressure (P) and temperature (T) (Tomioka and Miyahara 2017). Some of the early studies were pioneer in order to link the coexistence of various minerals with shock-impact events that have led to the formation of HP polymorphs in chondritic meteorites either by solid-solid reaction (Gillet et al. 2000; Beck et al. 2004; El Goresy et al. 2008, 2010; Bindi et al. 2017, 2020) or by crystallization of melts in shock veins (Miyahara et al. 2008, 2009). In some cases, static experiments were preferred to shock experiments to account for collisions of large asteroidal bodies or the passage of multiple shock waves through such bodies during multi-stage collisional events (Chen et al. 1996).

Among the several studies reporting the observation of high-pressure minerals in meteorites (e.g., El Goresy et al. 2000, 2001a, b, 2008, 2010; Tomioka and Miyahara 2017; Bindi et al. 2017, 2020; Tomioka et al. 2021), the discovery of metallic alloys has been of particular interest as these provide (1) direct information on differently O_2-depriveted portions of the Solar Nebula where alloys condensated, (2) a snapshot of the cooling history of the pristine chondritic material, and (3) a valid comparative model of core formation and chemical composition (McDonough and Sun 1995). Due to the different chemical compositions of the observed metallic particles found in meteorites, their relation with the bulk chemistry of the hosting meteorite along with textural observations has required a different interpretation. For instance, El Goresy and Chao (1976, 1977) reported the discovery of Fe-Ni-Cr particles in the basement rocks of Ries crater (Germany) that were attributed to a condensation process after vaporization of the impacting (carbonaceous) stony meteorite. This finding of metal particles was anticipated by the description of Co-, Cu-, and Ni-rich spheroids within impactites from the Barringer Meteorite Crater in Arizona by Kelly et al. (1974) explained on the basis of extensive chemical

* Correspondence: luca.bindi@unifi.it
[2]Dipartimento di Scienze della Terra, Università di Firenze, Via La Pira 4, I-50121 Florence, Italy
Full list of author information is available at the end of the article

reactions with the impacted target as well as Fe removal by oxidation and vaporization processes when meteorites pass through the terrestrial atmosphere. Palme and Wlotzka (1976) and El Goresy et al. (1978) reported the finding of a metal particle from the Ca, Al-rich inclusion of the Allende and Leoville meteorites markedly enriched in platinum group elements (PGE) and explained as result of condensation process from the Solar Nebula when not representative of pre-solar grains (i.e., Fremdlinge). Several studies have focused on the different Fe/Ni ratios of kamacite and taenite from stony meteorites referred to the different cooling histories (Reed 1964). More recently, the finding of metallic Fe coexisting with Fe-rich bridgmanite (hiroseite) in a shock vein of Suizhou meteorite (Bindi et al. 2020) has been reported as the first direct evidence in nature of redox-driven disproportionation reactions (Frost et al. 2004). Such discovery highlights the fact that (HP) mineral assemblages found in shocked meteorites can either have inherited the redox conditions of the portion of Solar Nebula where chondritic material formed (Stagno and Aulbach 2021) or have reached equilibrium within 10^{-1}–10^{0} seconds during the impact event (Ohtani et al. 2007; Beck et al. 2005; Xie and Sharp 2007) whose P, T, and chemical composition are influenced by the locally buffered oxygen fugacity (fo_2). On the other hand, studies conducted through molecular dynamic simulations have established a relation between the heliocentric distance and the redox conditions of the accreting bodies with the latter being more oxidized beyond 1.1-1.7 AU (Rubie et al. 2015).

Over this last decade, fundamental questions have been raised by the finding of metallic inclusions in the Khatyrka meteorite, a CV3 carbonaceous chondrite discovered in the Koryak mountains of Chukotka in Eastern Russia (Bindi et al. 2012; MacPherson et al. 2013). These particles were found to be Al-Cu(Ni)-Fe alloys with a quasiperiodic atomic arrangement, materials well studied for the last 35 years in the laboratory but exceedingly rare in nature (Shechtman et al. 1984; Levine and Steinhardt 1984; Bindi et al. 2009). The natural quasicrystals were then named icosahedrite ($Al_{63}Cu_{24}Fe_{13}$) and decagonite ($Al_{71}Ni_{24}Fe_5$; Bindi et al. 2011, 2015b), and recently, a first model of formation has been reported on the basis of their trace element contents (Tommasini et al. 2021).

The presence of stishovite, ahrensite, and a spinelloid phase reported in Khatyrka fragments (Hollister et al. 2014) as well as the presence of (redox) reaction rims (Lin et al. 2017) in the proximity of these particles were interpreted as evidence that the meteorite formed as result of a multi-stage process that started with the (1) condensation of Al-Cu-Fe from reduced portions of the Solar Nebula about 4.56 Gya and (2) experienced shock metamorphism induced by a hypervelocity impact with pressures exceeding at least 10 GPa and temperatures up to 1500 °C about < 600 Ma before (3) being ejected from its parent (K-type) asteroid 2–3 Ma ago (Meier et al. 2018). Moreover, the recent discovery of a CO-type chondritic spherule from the Nubian Desert, Sudan, containing the same assemblage of aluminum, iron, and copper and with a morphology remarkably similar to Khatyrka, provided further support and independent evidence that these samples were formed in outer space (Suttle et al. 2019).

Figure 1 is a cartoon summarizing the state of art for the metallic inclusions in Khatyrka meteorite. Several experimental studies were conducted at the aim both to reproduce shock-impact events to verify whether extraterrestrial quasicrystals would form and to test the stability of Al-Cu-Fe quasicrystal as function of pressure and temperature (see Table 1).

The first set of dynamic compression experiments successfully resulted in the formation of both icosahedral Al-Cu-Fe QC (Asimow et al. 2016; Oppenheim et al. 2017a; Hu et al. 2020) and decagonal QC (Oppenheim et al. 2017b) by performing shock experiments.

Studies aimed to test the stability of icosahedrite were carried out by Stagno et al. (2014, 2015, 2017) using both in situ multi anvil (MA) and diamond anvil cell (DAC) techniques assisted by synchrotron radiation X-ray diffraction (XRD) at room/high temperature. The results from these studies showed that (1) synthetic icosahedrite remains stable without any transformation to approximant phases over a wide P range from 3 to 42 GPa and T up to 1600 °C, (2) it exhibits a negligible effect of pressure on the volumetric thermal expansion properties, and (3) the quasiperiodic order of icosahedrite is retained up to 51.3 GPa. Importantly, it has been shown that pressure acts to stabilize the icosahedral symmetry at temperatures much higher than previously reported and that direct solidification of AlCuFe QCs from an unusually Al-Cu-rich melt is possible but it is limited to a narrow temperature range (Stagno et al. 2017). However, the possibility that icosahedrite could form in nature and survived at elevated pressures and temperature conditions cannot be excluded as this relies on the experimental investigation of its structural behavior and potential decomposition products at high pressures.

As motivation of this study, there is evidence that heavily shocked ordinary chondrites, classified into shock stage S6, have experienced pressures up to ~ 75 GPa as confirmed by the presence of high-pressure minerals (Stöffler et al. 2018). Hence, the extension of pressure ranges up to ~ 70 GPa and beyond is important to understand the icosahedrite stability in shocked meteorites.

Therefore, we report in situ angle-dispersive X-ray powder diffraction (XRD) measurements on synthetic icosahedrite to extend the investigation of the interplanar

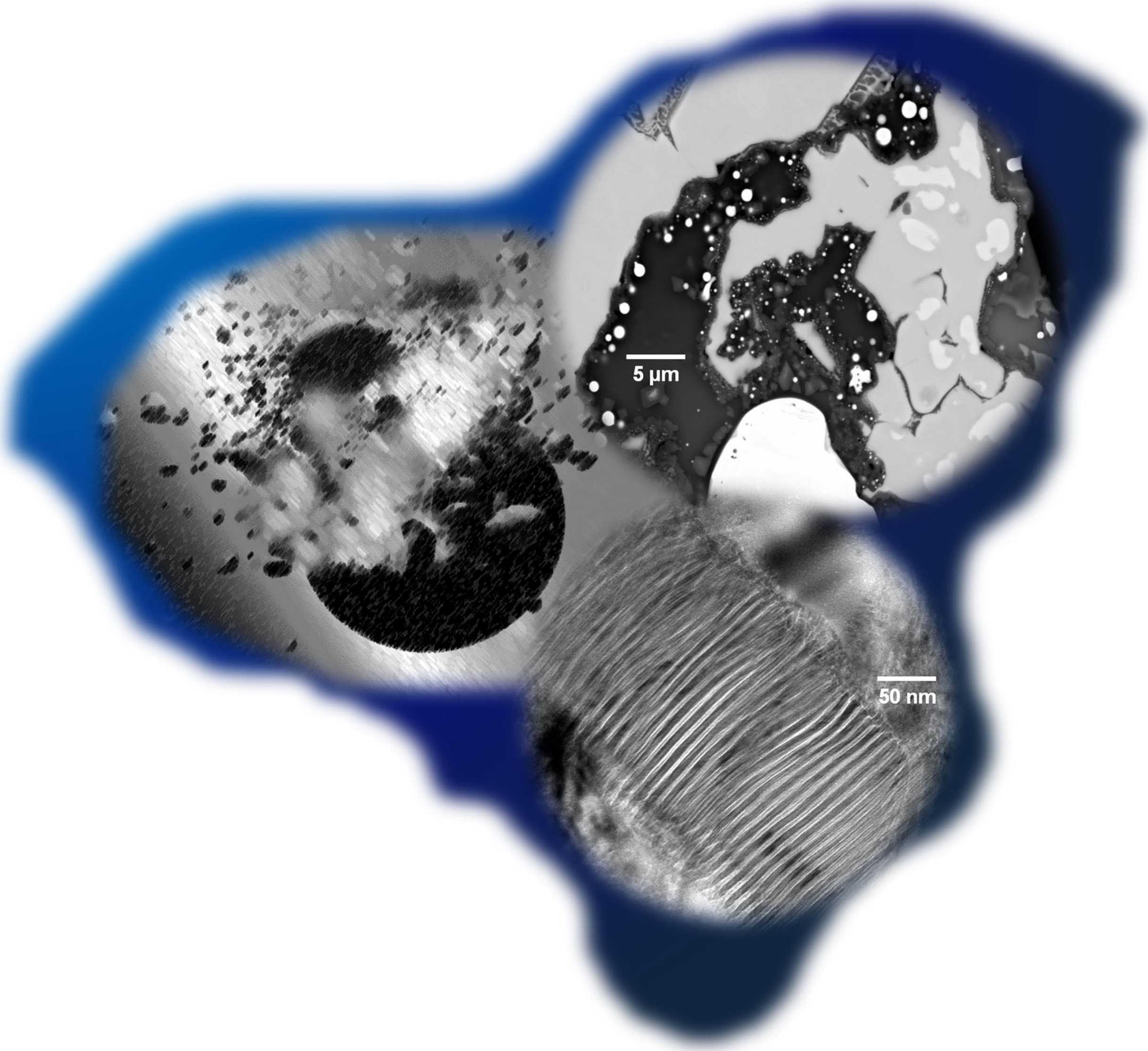

Fig. 1 Cartoon summarizing details of the Khatyrka meteorite. Top-left: schematic sketch of an asteroidal collision in outer space; top-right: SEM-BSE image of Grain 126A of the Khatyrka meteorite. Brighter phases indicate Cu-Al-alloys and Fe-droplets, while darker phases are silicates and oxides (see Lin et al. 2017 for more explanations); bottom: TEM image of Grain 125 of the Khatyrka meteorite showing "ladders" composed by ringwoodite and amorphous silica (see Hollister et al. 2014 for more explanations)

distances at pressures up to about 75 GPa at ambient temperature. Our results are integrated with data by Takagi et al. (2015) on the compression behavior of icosahedral $Al_{65}Cu_{22}Fe_{13}$ to better understand the possible evolution of icosahedrite at megabar pressures adopting a univocal compression model.

2 Materials and methods

The synthetic quasicrystal used as starting material in this study is the same as that used by Stagno et al. (2015), and it was previously characterized by SEM and XRD measurements and showed to have the formula $Al_{63}Cu_{24}Fe_{13}$ (Bancel 1999) plus minor amounts of cupalite, (Cu, Fe)Al. The advantage of using this starting material is that its composition can be considered the analog of icosahedrite (Bindi et al. 2011). After extracting a small fragment from the synthetic single crystal, a small chip was crushed to form a platelet. A small platelet with a diameter of approximately 60 μm was loaded into the sample chamber of a symmetric diamond anvil cell with flat anvils of 300-μm size culet and rhenium gasket as sample chamber with a 150-μm diameter hole. In situ angle-dispersive X-ray diffraction (ADXRD) measurements were performed at high pressure at the 13ID-

Table 1 Bulk modulus (B_0) and its pressure derivative (B'_0) for Al-Cu-Fe alloys and end-members

Composition	Technique	*P* (GPa)	B_0	B'_0	References
i-$Al_{62}Cu_{25.5}Fe_{12.5}$	EDXD	35	139 (6)	2.7	Sadoc et al. (1994)
i-$Al_{62}Cu_{25.5}Fe_{12.5}$	EDXD	33.6	155 (10)	2	Lefebvre et al. (1995)
p-$Al_{62.8}Cu_{26}Fe_{11.2}$	EDXD	29.8	175 (16)	2	Lefebvre et al. (1995)
r-$Al_{64}Cu_{24}Fe_{12}$	EDXD	35	175 (16)	2	Lefebvre et al. (1995)
i-$Al_{65}Cu_{22}Fe_{13}$	ADXD	72	131 (7)	4 (fixed)	Takagi et al. (2015)
i-$Al_{63}Cu_{24}Fe_{12}$	ADXD	75.8	121 (8)	3.68 (4)	This study
Al	ADXD	144.3	76.3 (1.1)	4.16 (5)	Dewaele et al. (2004)
Cu	ADXD	144.3	135.1 (1.1)	4.91 (5)	Dewaele et al. (2004)
Fe	EDXD	300	165 (4)	5.33 (9)	Mao et al. (1990)

EDXD stays for energy-dispersive X-ray diffraction, while ADXD stays for angle-dispersive X-ray diffraction

D beamline (GSECARS) of the Advanced Photon Source in Argonne (Illinois). Neon was loaded as the pressure medium, and the DAC was mounted on a motor-driven stage with the tungsten carbide (WC) seat on the downstream side and the cubic boron nitride (c-BN) seat on the upstream side. A focused monochromatic 30-keV X-ray beam with a wavelength of 0.4133 Å and a sample-to-detector distance of ~ 296 mm was used. Diffraction patterns were collected on a MarCCD-165 detector with exposure time of 15 s. Pressure was measured using the thermal equation of state (EoS) of Ne used as pressure medium (Hemley et al. 1989). The collected data were processed using FIT2D software (Hammersley 1998), and the *d*-spacing relative to each reflection was accurately determined using PeakFit software.

3 Results and discussion

The collected most representative diffraction data of synthetic icosahedrite are shown in Fig. 2 as function of pressure, while Table 2 shows the *d*-spacing at different pressures using the two-integer indices (Janot 1994; Lu et al. 2001) along with the estimated pressures from the equation of state of Ne. The peaks were indexed according to Bindi et al. (2011), and the *d*-spacing was

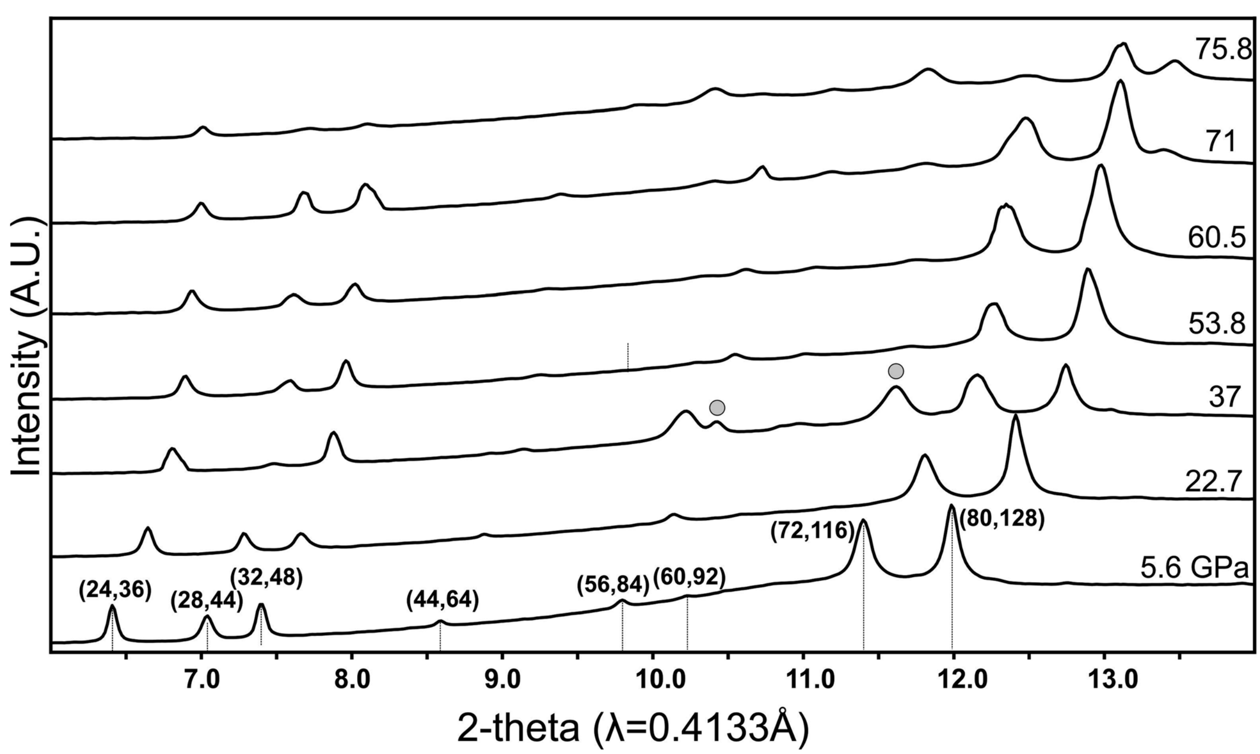

Fig. 2 Pressure effect on selected interplanar spacings (Å-angstrom) of the synthetic icosahedrite under quasi-hydrostatic conditions (Ne pressure medium). Symbols: diamonds and triangles indicate previous runs (Stagno et al. 2015). Squares are experiments from this study

Table 2 Pressure dependences of *d*-spacings (Å) and a_{6D} (Å) from the characteristic peaks

P_{Ne} (GPa)	V (Å^3)	a_{6d}	(8,4)	(12,16)	(24,36)	(28,44)	(32,48)	(44,64)	(56,84)	(60,92)	(72,116)	(80,128)
0.0	2020.96	12.6431	8.94	5.53	3.750	3.410	3.240	2.799	2.451	2.350	2.108	2.006
5.0	1938.85	12.4695	8.82	5.44	3.698	3.368	3.201	2.760	2.420	2.319	2.080	1.979
5.6	1929.35	12.4491	8.80	5.45	3.696	3.366	3.203	2.759	2.420	2.319	2.081	1.979
21.8	1746.67	12.0431	8.52	5.26	3.566	3.252	3.092	2.669	2.339	2.239	2.009	1.912
22.7	1747.89	12.0459	8.52	5.27	3.571	3.251	3.094	2.665	2.338	2.241	2.012	1.912
35.4	1637.86	11.7876	8.33	5.16	3.495	3.181	3.021	2.609	2.326	2.194	1.971	1.872
37.0	1611.29	11.7235	8.29	5.14	3.478	3.164	3.007	2.593	2.320	2.185	1.952	1.862
42.8	1617.61	11.7388	8.30	5.13	3.479	3.161	3.009	2.593	2.321	2.180	1.954	1.858
40.0	1608.28	11.7162	8.28	5.13	3.476	3.163	3.007	2.594	2.320	2.183	1.953	1.858
40.0	1606.81	11.7126	8.28	5.14	3.477	3.168	3.007	2.593	2.320	2.183	1.954	1.862
51.0	1571.31	11.6257	8.22	5.07	3.447	3.133	2.986	2.573	2.305	2.158	1.941	1.846
53.8	1562.72	11.6045	8.21	5.05	3.437	3.127	2.977	2.562	2.303	2.153	1.935	1.840
56.8	1556.76	11.5897	8.19	5.04	3.427	3.118	2.968	2.558	2.296	2.147	1.930	1.835
60.5	1528.91	11.5202	8.15	5.04	3.414	3.113	2.956	2.550	2.287	2.140	1.921	1.829
63.5	1520.63	11.4994	8.13	5.02	3.406	3.106	2.949	2.541	2.278	2.137	1.916	1.824
66.5	1507.03	11.4650	8.11	5.01	3.397	3.098	2.940	2.533	2.280	2.129	1.911	1.819
68.0	1501.09	11.4499	8.10	4.99	3.396	3.093	2.936	2.533	2.281	2.128	1.908	1.816
71.0	1484.92	11.4087	8.07	4.98	3.386	3.085	2.926	2.526	2.277	2.119	1.901	1.811
71.5	1481.15	11.3990	8.06	4.97	3.391	3.095	2.935	–	2.281	2.120	1.906	1.815
75.8	1453.00	11.3263	8.01	4.95	3.380	3.075	2.925	–	2.277	2.116	1.897	1.812
74.5	1452.88	11.3260	8.01	4.96	3.375	3.076	2.920	2.515	2.271	2.115	1.897	1.806
74.5	1449.65	11.3176	8.00	4.97	3.375	3.073	2.916	2.516	2.278	2.119	1.902	1.805
54.0	1570.54	11.6238	8.22	5.08	3.453	3.141	2.986	2.575	–	–	1.944	1.846
27.8	1712.36	11.9637	8.46	–	3.565	3.237	3.077	–	–	–	–	–

determined by fitting each diffraction peak using a Gaussian formula within an uncertainty of less than 0.01 Å. The effect of pressure on the *d*-spacing is shown in Fig. 3 with P determined by the EoS of Ne. According to our results, seven out of eight interplanar distances show a similar linear compression behavior, unlike (8,4) that appears more compressible over the P range of investigation. This is more evident in Fig. 4 where the pressure dependence of the lattice parameter a_{6D} is plotted up to the maximum pressure of ~ 76 GPa defined as,

$$a_{6D} = d\sqrt{\frac{N + M\tau}{2(2+\tau)}} \tag{1}$$

where d is the *d*-spacing in Å, N and M are the Cahn indices for which the *d*-spacing is experimentally determined (i.e., (8,4) in this case), and τ is the golden ratio, (1+√5)/2 (Steurer and Deloudi 2009). The six-dimensional lattice parameter, with respect to the zero-P parameter by Bindi et al. (2011), is shown to gradually decrease with increasing pressure (Fig. 4) well in agreement with data by Stagno et al. (2015) providing, therefore, a significant evidence of reproducibility of the obtained results that reflects also the accuracy of the performed experiments in both compression and decompression. The estimated reduction of the lattice parameter from the ambient pressure value of 12.64 Å to 75.8 GPa is about 10.4% implying a constant compressibility behavior as previously observed up to 50 GPa. No clear evidences of either structural phase transitions or amorphization were observed within the investigated pressure range as it can be also seen in Fig. 2. Figure 4 also shows data by Takagi et al. (2015) collected by in situ ADXRD but on synthetic $Al_{65}Cu_{22}Fe_{13}$. In their study, these authors reported no substantial changes in the XRD profile relative to five characteristic peaks up to 104 GPa. These are the (24,36), (28,44), (32,48), (72,116), and (80,128) for which the least anisotropy was also observed in our measurements in case of the synthetic analog of icosahedrite, $Al_{63}Cu_{24}Fe_{13}$. No information was derived for the most anisotropic (8,4) reflection, which is likely the reason of the little difference with respect to the study by Stagno et al. (2015).

The data were fitted to both Murnaghan and Birch-Murnaghan EoS (Angel et al. 2014). The former model

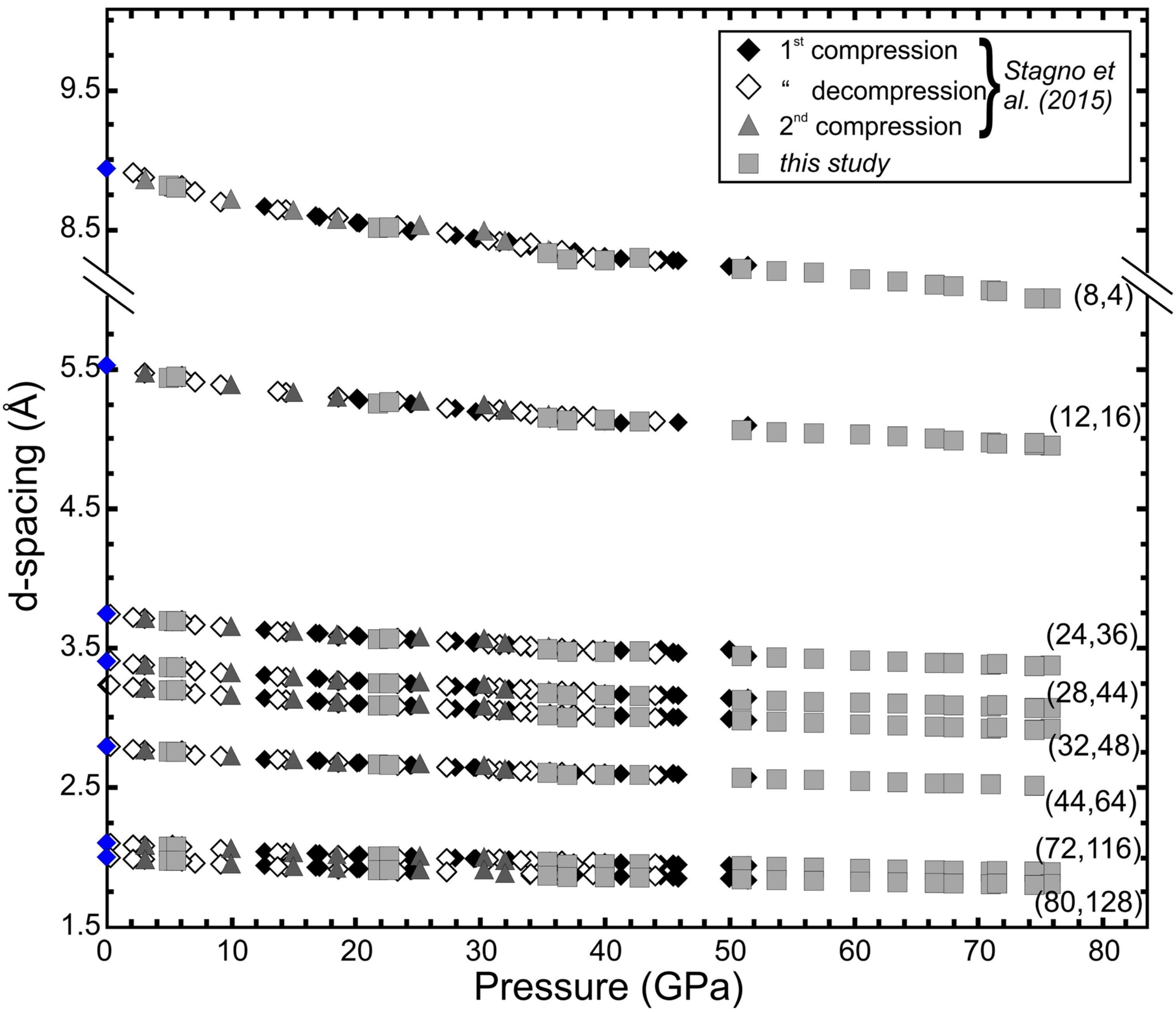

Fig. 3 Representative powder X-ray diffraction patterns of i-QC collected at room temperature in angle-dispersive mode (wavelength of 0.4133 Å) as function of pressure. Filled gray circles refer to Au used as a pressure marker. The diffraction peaks are indexed using Cahn indices (*N*, *M*) following the scheme proposed by Janot (1994)

allows a direct comparison with the previous experimental data from literature (see Table 1) and results in a bulk modulus of 121(8) GPa (B_0' of 3.68 ± 4), which is close with the 113.7 GPa (B_0' of 4.22) obtained for the same QC compressed to 50 GPa (Stagno et al. 2015). As a consequence of the observed consistency between the present data and those by Stagno et al. (2015), we can fit successfully all of them to the same EoS and obtain a B_0 of 120(2) GPa and B_0' of 3.87(14). These EoS parameters are slightly smaller than 139 GPa (B_0' of 2.7) in case of icosahedral $Al_{62}Cu_{25.5}Fe_{12.5}$ by Sadoc et al. (1994), 155 GPa (B_0' of 2.0) by Lefebvre et al. (1995), and close to 120 GPa (B_0' of 5) for decagonal $Al_{72}Ni_{20}Co_8$ (Hasegawa et al. 1999). A fit of our data to the third-order Birch-Murnaghan EoS produces little negligible differences (B_0 116 ± 3, B_0' of 4.39 ± 17). Noteworthy, we refer to the decagonal phase since, at present, this is the only available data on the physical properties of decagonal QC with composition very close to that found in nature, $Al_{71}Ni_{24}Fe_5$, for which a HP origin has been proposed (Bindi et al. 2015a, b).

Interestingly, Takagi et al. (2015) noted a slightly volume shift between 72 and 75 GPa beyond which they claimed that the QC would transform to an approximant phase. This consideration is supported, in their opinion, by the appearance of small unknown peaks at 2θ of ~ 8.5° and 10.6° for (λ = 0.41441 Å). Therefore, their data were fitted to 72 GPa using a third-order Birch-Murnaghan EoS to

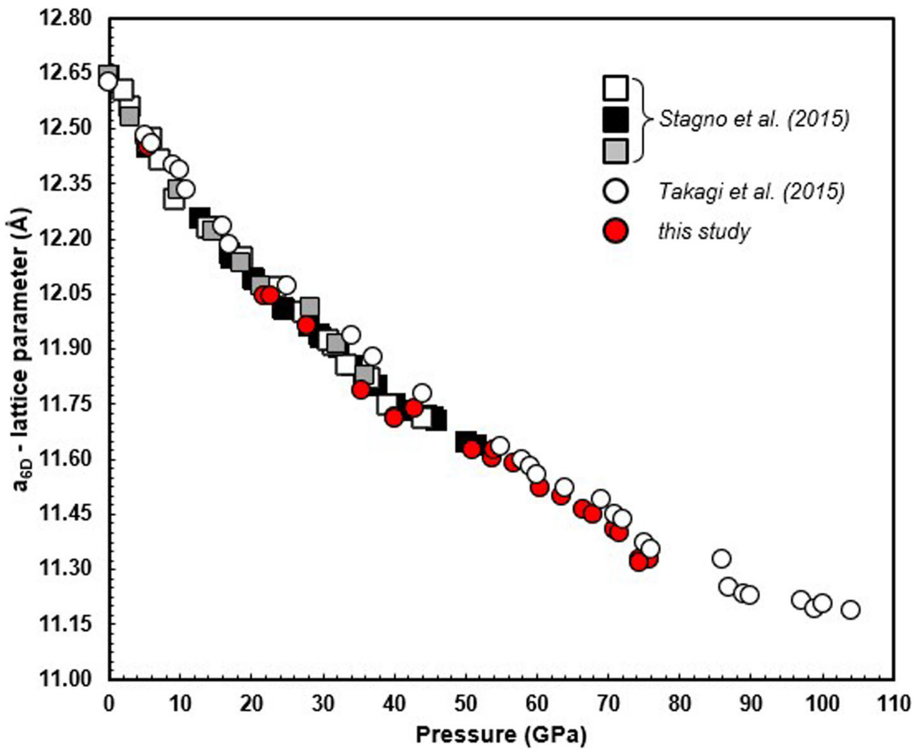

Fig. 4 Variation of the lattice parameter as function of pressure compared with similar studies on $Al_{63}Cu_{24}Fe_{13}$ (Stagno et al. 2015) and $Al_{65}Cu_{22}Fe_{13}$ (Takagi et al. 2015). The zero-P volume is from Bindi et al. (2011)

give a bulk modulus of 131(7) GPa (B_0' of 4 as fixed value). A second EoS fit for volume-P data collected from 74 to 104 GPa provided a higher bulk modulus like 170(40) GPa (B_0' of 4 as fixed value). Such difference was proposed to be caused by the different compressional behavior of i-QC and an approximant phase, although no sufficient evidence exists that such phase transformation could occur. For instance, it cannot be excluded that the peaks reported as unknown could be representative of weak reflections of the i-QC that appears visible as result of preferred orientation upon compression (similar peaks also were observed within a lower P range for similar compositions by Lefebvre et al. 1995). The unknown peak that Takagi et al. (2015) noted at 10.6° = ~ 2.24 Å would correspond to the reflection (56,84) of the i-QC (Bindi et al. 2009, 2011). Further, it is not surprising that the compressibility reported by Stagno et al. (2015) is slightly higher than that obtained by Takagi et al. (2015) as the latter determined the EoS from the least compressible *d*-spacings of i-QC; on the contrary, Stagno et al. (2015) performed a high-resolution investigation of the icosahedral structure by monitoring the behavior in the high *d*-spacing region that included peaks (12,16) at 5.53 Å and (8,4) at 8.94 Å. The *d*-spacing referred to this latter reflection manifested a more evident anisotropic compressional behavior resulting, therefore, in a lower bulk modulus. On the other hand, first-order phase transitions would appear visible through the variation of the *d*-spacing as function of P. Figure 3 shows a continuous decrease of *d*-spacing as P increases up to 75.8 GPa. Therefore, we fit the data by Stagno et al. (2015) up to 72 GPa along with those by Takagi et al. (2015) up to 104 GPa with only a unique EoS. The obtained bulk modulus of 121(3) GPa (B_0' of 3.87 ± 12) using a Murnaghan EoS fitting model is consistent with the EoS parameters used to fit our data up to 75 GPa. Fitted to a third-order Birch-Murnaghan EoS, we obtain a bulk modulus of 117(3) GPa (B_0' of 4.45 ± 15), which is again consistent with the previous fit by Stagno et al. (2015). Both fitting models are showed in Fig. 5 with an imperceptible difference between them. Data from literature are also shown by comparison. In particular, the compressibility of icosahedral $Al_{62}Cu_{25.5}Fe_{12.5}$ determined by Sadoc et al. (1994) and Lefebvre et al. (1995) has been extrapolated up to 104 GPa assuming that no phase transition occurs for this composition by analogy with those investigated here. Both curves are quite consistent with the experimental measurements although a little shift is likely due to, again, the fact that the lattice parameter was determined by the less compressible *d*-spacing. In addition, loss of hydrostaticity could have occurred

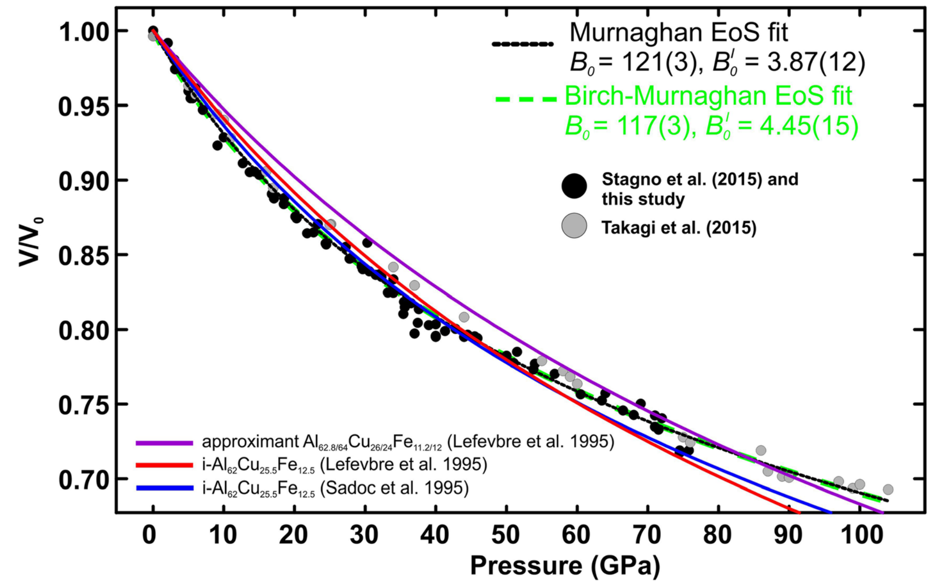

Fig. 5 Pressure-volume data for i-$Al_{64}Cu_{23}Fe_{13}$ from this study (black circles) and Takagi et al. (2015; empty circles) fitted using both a Murnaghan (black dotted line) and Birch-Murnaghan EOS (dashed green line). Our fit is compared with previous studies by Sadoc et al. (1994) and Lefebvre et al. (1995) both for icosahedral $Al_{62}Cu_{25.5}Fe_{12.5}$ and for one approximant phase with composition $Al_{64}Cu_{24}Fe_{12}$ (Lefebvre et al. 1995). The curves obtained from these previous studies are extrapolated up to 104 GPa assuming that no structural phase transformation occurs

because of the use of silicon oil as pressure medium. Importantly, the extrapolated V/V_0 is shown also for the rhombohedral and pentagonal approximant phases by Lefebvre et al. (1995) where periodic approximant refers to a crystalline solid with similar chemical composition to a quasicrystal, but whose atomic arrangement is slightly distorted so that the symmetry conforms to the conventional laws of three-dimensional crystallography. These phases, although described to have a slightly different chemical composition, resulted to have the same physical behavior at high P reflected by the same EoS parameters. Interestingly, these approximant phases are shown to undergo a volumetric reduction under compression that is apparently lower than the QC phase. Therefore, we are confident that no phase transition occurred at P > 72 GPa within the Al-Cu-Fe system investigated to date. This evidence raises important questions on the stability also of approximant phases on extraterrestrial bodies that experienced shock-impact events. The recent findings of a quasicrystal with 10-fold symmetry, decagonite, with composition $Al_{71}Ni_{24}Fe_5$ (Bindi et al. 2015a, b) and its approximant, proxidecagonite (Bindi et al. 2018), in the same Khatyrka meteorite suggest the possibility that P-T conditions might play a key role in determining the most energetically stable atomic configuration. To date, however, no approximant to icosahedrite has been found that support the possibility that this phase transition might require extremely high P-T conditions never explored so far in experiments.

At the present, both dynamic and static compression experiments have revealed the structural stability of i-QC. Both icosahedral Al-Cu-Fe quasicrystals (Asimow et al. 2016; Oppenheim et al. 2017a; Hu et al. 2020) and decagonal quasicrystals (Oppenheim et al. 2017b) were reported as run products of shock experiments during which shock pressures up to 35 GPa were generated with T as high as 400 °C within less than 1 μs. These experiments succeeded in reproducing both the textural contacts between the quasicrystalline phases and the Al-Cu-Fe alloys as well as their chemical composition as in the Khatyrka meteorite. More importantly, the finding of quasicrystals incorporating additional elements like Cr and Ni to the known Al-Cu-Fe, as well as the variability of the Al/Cu and Cu/Fe atomic ratios, represent an important evidence that quasicrystals do form during impact and keep their structural stability under more complex chemical environments than previously thought.

Static experiments carried out in the diamond anvil cell, in particular, have extended our knowledge of the behavior of synthetic icosahedrite up to megabar pressures. The effect of temperature has been investigated through either laser heating in DAC or multi anvil experiments. While the former helped to verify the structural stability of the i-QC during heating up to ~ 1850 °C and upon cooling/quench, experiments performed with the large volume press helped to shed light on the kinetics versus thermodynamic stability of the QC. Stagno et al. (2017) showed experimentally that icosahedrite can be stable for hours under hydrostatic compression at HT in the presence of additional minerals like cupalite, khatyrkite, and stolperite, similarly to what are found in nature. The experimental observation of the coexistence of synthetic icosahedrite along with an Al-Cu-Fe melt (plus additional phases) proves that icosahedrite can survive at those high P-T conditions at which shock glassy veins containing high-P polymorphs were proposed to form. We are confident that important steps forward have been done through experimental studies that demonstrate both the kinetics and thermodynamic stability of Al-Cu-Fe QCs, expanding, therefore, their potential occurrence through space and time.

4 Conclusions

We presented the results of experiments conducted at P up to ~ 76 GPa using the DAC technique that confirms the stability of icosahedrite at high P. Our results appear consistent with previous data collected up to 50 GPa and show a linear decrease of the *d*-spacing with the exception for the (8,4) reflection, as never observed to the present, for which the calculated volume reduction is about 10% with respect to the V_0. Our data were, therefore, integrated with those previously published by Takagi et al. (2015), who claimed for the transition of the i-QC to an approximant phase at 72–75 GPa. Based on a re-fit of these data along with those by Stagno et al. (2015) to a unique EoS fit model, we propose that icosahedrite can retain its structure up to megabar pressures. This extended P range, further accompanied by the stability of i-QC at elevated T representative of shock impacts, rules out the possibility to find Al-Cu-Fe approximant phases in the Khatyrka meteorite.

Acknowledgements

Portions of this work were performed at GeoSoilEnviroCARS (The University of Chicago, Sector 13), Advanced Photon Source (APS), Argonne National Laboratory. GeoSoilEnviroCARS is supported by the National Science Foundation – Earth Sciences (EAR – 1634415) and Department of Energy-GeoSciences (DE-FG02-94ER14466). This research used resources of the Advanced Photon Source, a U.S. Department of Energy (DOE) Office of Science User Facility operated for the DOE Office of Science by Argonne National Laboratory under Contract No. DE-AC02-06CH11357. We are grateful to Sergey Tkachev and Vitali Prakapenka (GSECARS) for their help during the experiments. We are particularly delighted to participate to the special issue honoring Ahmed El Goresy. His numerous discoveries of shock-induced high-pressure phases in meteorites and samples from terrestrial impact craters made possible to detect several unusual mineral assemblages. With his work, Ahmed significantly contributed to a better understanding of cosmochemical processes in the early solar system.

Authors' contributions

VS and LB proposed the topic, conceived, and designed the study. VS carried out the experimental study. VS and LB analyzed the data and helped in their interpretation. ST and AK collaborated with the corresponding author in the construction of manuscript. All authors read and approved the final manuscript.

Funding

This work benefited from partial support by "Fondi di Ateneo 2019" of the Sapienza University, Italy to V.S. The research was also in part funded by MIUR-PRIN2017, project "TEOREM deciphering geological processes using Terrestrial and Extraterrestrial ORE Minerals," prot. 2017AK8C32 (PI: Luca Bindi).

Availability of data and materials

The dataset supporting the conclusions of this article is included within the article and its additional file.

Declarations

Competing interests

The authors declare that they have no competing interest.

Author details

[1]Dipartimento di Scienze della Terra, Università La Sapienza, P.zle Aldo Moro 5, I-00185 Rome, Italy. [2]Dipartimento di Scienze della Terra, Università di Firenze, Via La Pira 4, I-50121 Florence, Italy. [3]Institute of Materials Structure Science, High Energy Accelerator Research Organization (KEK), Ibaraki, Japan. [4]Division of Earth Evolution Sciences, Graduate School of Life and Environmental Sciences, University of Tsukuba, Ibaraki, Japan.

Received: 13 January 2021 Accepted: 25 March 2021
Published online: 20 April 2021

References

Angel RJ, Gonzalez-Platas J, Alvaro M (2014) EosFit7c and a Fortran module (library) for equation of state calculations. Zeit Kristallogr 229:405–419

Asimow PD, Lin C, Bindi L, Ma C, Tschauner O, Hollister LS, Steinhardt PJ (2016) Shock synthesis of quasicrystals with implications for their origin in asteroid collisions. Proc Nat Acad Sci USA 113(26):7077–7081. https://doi.org/10.1073/pnas.1600321113

Bancel PA (1999) Order and disorder in icosahedral alloys. Quasicrystals. In: DiVincenzo DP, Steinhardt PJ (eds) Series on directions in condensed matter physics, vol 16. World Scientific, Singapore, pp 17–55

Beck P, Gillet P, El Goresy A, Mostefaoui S (2005) Timescales of shock processes in chondritic and martian meteorites. Nature 435(7045):1071–1074. https://doi.org/10.1038/nature03616

Beck P, Gillet P, Gautron L, Daniel I, El Goresy A (2004) A new natural high-pressure (Na, Ca)-hexaluminosilicate [$(Ca_xNa_{1-x})Al_{3+x}Si_{3-x}O_{11}$] in shocked Martian meteorites. Earth Planet Sci Lett 219(1-2):1–12. https://doi.org/10.1016/S0012-821X(03)00695-2

Bindi L, Chen M, Xie X (2017) Discovery of the Fe-analogue of akimotoite in the shocked Suizhou L6 chondrite. Sci Rep 7(1):42674. https://doi.org/10.1038/srep42674

Bindi L, Eiler JM, Guan Y, Hollister LS, MacPherson GJ, Steinhardt PJ, Yao N (2012) Evidence for the extra-terrestrial origin of a natural quasicrystal. Proc Nat Acad Sci USA 109(5):1396–1401. https://doi.org/10.1073/pnas.1111115109

Bindi L, Pham J, Steinhardt PJ (2018) Previously unknown quasicrystal periodic approximant found in space. Sci Rep 8(1):16271. https://doi.org/10.1038/s41598-018-34375-x

Bindi L, Shim S-H, Sharp TG, Xie X (2020) Evidence for the charge disproportionation of iron in extraterrestrial bridgmanite. Sci Adv 6:eaay7893

Bindi L, Steinhardt PJ, Yao N, Lu PJ (2009) Natural quasicrystals. Science 324(5932):1306–1309. https://doi.org/10.1126/science.1170827

Bindi L, Steinhardt PJ, Yao N, Lu PJ (2011) Icosahedrite, $Al_{63}Cu_{24}Fe_{13}$, the first natural quasicrystal. Am Mineral 96(5-6):928–931. https://doi.org/10.2138/am.2011.3758

Bindi L, Yao N, Lin C, Hollister LS, Andronicos CL, Distler VV, Eddy MP, Kostin A, Kryachko V, MacPherson GJ, Steinhardt WM, Yudovskaya M, Steinhardt PJ (2015a) Natural quasicrystal with decagonal symmetry. Sci Rep 5(1):9111. https://doi.org/10.1038/srep09111

Bindi L, Yao N, Lin C, Hollister LS, Andronicos CL, Distler VV, Eddy MP, Kostin A, Kryachko V, MacPherson GJ, Steinhardt WM, Yudovskaya M, Steinhardt PJ (2015b) Decagonite, $Al_{71}Ni_{24}Fe_5$, a quasicrystal with decagonal symmetry from the Khatyrka CV3 carbonaceous chondrite. Am Mineral 100(10):2340–2343. https://doi.org/10.2138/am-2015-5423

Chen M, Sharp TG, El Goresy A, Wopenka B, Xie X (1996) The majorite-pyrope + magnesiowüstite assemblage: constraints on the history of shock veins in chondrites. Science 271(5255):1570–1573. https://doi.org/10.1126/science.271.5255.1570

Dewaele A, Loubeyre P, Mezouar M (2004) Equations of state of six metals above 94 GPa. Phys Rev B 70(9):094112. https://doi.org/10.1103/PhysRevB.70.094112

El Goresy A, Chao ECT (1976) The discovery of Fe-Cr-Ni veinlets below the crater bottom. Earth Planet Sci Lett 31(3):330–340. https://doi.org/10.1016/0012-821X(76)90114-X

El Goresy A, Chao ECT (1977) Discovery, origin, and significance of Fe-Cr-Ni veinlets in the compressed zone of the 1973 Ries research drill core. Geol Bavar 75:305–321

El Goresy A, Chen M, Dubrovinsky L, Gillet P, Graup G (2001a) An ultradense polymorph of rutile with seven coordinated titanium from the Ries crater. Science 293(5534):1467–1470. https://doi.org/10.1126/science.1062342

El Goresy A, Chen M, Gillet P, Dubrovinsky L, Graup G, Ahuja R (2001b) A natural shock-induced dense polymorph of rutile with a-PbO_2 structure in the suevite from the Ries crater in Germany. Earth Planet Sci Lett 192(4):485–495. https://doi.org/10.1016/S0012-821X(01)00480-0

El Goresy A, Dera P, Sharp TG, Prewitt CT, Chen M, Dubrovinsky L, Wopenka B, Boctor NZ, Hemley RJ (2008) Seifertite, a dense orthorhombic polymorph of silica from the Martian meteorites Shergotty and Zagami. Eur J Mineral 20(4): 523–528. https://doi.org/10.1127/0935-1221/2008/0020-1812

El Goresy A, Dubrovinsky L, Gillet P, Graup G, Chen M (2010) Akaogiite: an ultra-dense polymorph of TiO_2 with the baddeleyite-type structure, in shocked garnet gneiss from the Ries Crater, Germany. Am Mineral 95(5-6):892–895. https://doi.org/10.2138/am.2010.3425

El Goresy A, Dubrovinsky L, Sharp TG, Saxena SK, Chen M (2000) A monoclinic post-stishovite polymorph of silica in the Shergotty meteorite. Science 288(5471):1632–1634. https://doi.org/10.1126/science.288.5471.1632

El Goresy A, Nagel K, Ramdohr P (1978) Fremdlinge and their noble relatives. In: Lunar and planetary science conference, 9th, Houston, Tex., March 13-17, 1978, proceedings, vol 1. Pergamon Press, Inc., New York, pp 1279–1303 (A79-39107 16-91)

Frost DJ, Liebske C, Langenhorst F, McCammon CA (2004) Experimental evidence for the existence of iron-rich metal in the Earth's lower mantle. Nature 428(6981):409–412. https://doi.org/10.1038/nature02413

Gillet P, Chen M, Dubrovinsky L, El Goresy A (2000) Natural $NaAlSi_3O_8$-hollandite in the shocked Sixiangkou meteorite. Science 287(5458):1633–1636. https://doi.org/10.1126/science.287.5458.1633

Hammersley AP (1998) ESRF internal report, ESRF98HA01T, FIT2D V9.129 reference manual V3.1

Hasegawa M, Tsai AP, Yagi T (1999) Stability and strain of decagonal Al-Ni-Co quasicrystal under high pressure up to 70 GPa. Phil Mag Lett 79(9):691–698. https://doi.org/10.1080/095008399176733

Hemley RJ, Zha CS, Jephcoat AP, Mao HK, Finger LW, Cox DE (1989) X-ray diffraction and equation of state of solid neon to 110 GPa. Phys Rev B 39(16): 11820–11827. https://doi.org/10.1103/PhysRevB.39.11820

Hollister LS, Bindi L, Yao N, Poirier GR, Andronicos CL, MacPherson GJ, Lin C, Distler VV, Eddy MP, Kostin A, Steinhardt WM, Yudovskaya M, Eiler JM, Guan Y, Clarke JJ, Steinhardt PJ (2014) Impact-induced shock and the formation of natural quasicrystals in the early solar system. Nat Comm 5:3040

Hu J, Asimow PD, Ma C, Bindi L (2020) First synthesis of a unique icosahedral phase from the Khatyrka meteorite by shock recovery experiment. IUCrJ 7(3): 434–444. https://doi.org/10.1107/S2052252520002729

Janot C (1994) Quasicrystals: a primer. Oxford Univ. Press, Oxford

Kelly WR, Holdsworth E, Moore CB (1974) The chemical composition of metallic spheroids and metallic particles within impactite from Barringer Meteorite Crater, Arizona. Geoch Cosmochim Acta 38(4):533–543. https://doi.org/10.1016/0016-7037(74)90039-8

Lefebvre S, Bessiére M, Calvayrac Y, Itie JP, Polian A, Sadoc A (1995) Stability of icosahedral Al-Cu-Fe and two approximant phases under high pressure up to 35 GPa. Phil Mag B 72(1):101–113. https://doi.org/10.1080/13642819508239067

Levine D, Steinhardt PJ (1984) Quasicrystals: a new class of ordered structures. Phys Rev Lett 53(26):2477–2480. https://doi.org/10.1103/PhysRevLett.53.2477

Lin C, Hollister LS, MacPherson GJ, Bindi L, Ma C, Andronicos CL, Steinhardt PJ (2017) Evidence of cross-cutting and redox reaction in Khatyrka meteorite reveals metallic-Al minerals formed in outer space. Sci Rep 7(1):1637. https://doi.org/10.1038/s41598-017-01445-5

Lu PJ, Deffeyes K, Steinhardt PJ, Yao N (2001) Identifying and indexing icosahedral quasicrystals from powder diffraction patterns. Phys Rev Lett 87: 275507–1–275507–4

MacPherson GJ, Andronicos CL, Bindi L, Distler VV, Eddy MP, Eiler JM, Guan Y, Hollister LS, Kostin A, Kryachko V, Steinhardt WM, Yudovskaya M, Steinhardt PJ (2013) Khatyrka, a new CV3 find from the Koryak Mountains, Eastern Russia. Meteorit Planet Sci 48(8):1499–1514. https://doi.org/10.1111/maps.12170

Mao HK, Wu Y, Chen LC, Shu JF, Jephcoat AP (1990) Static compression of iron to 300 GPa and Fe Ni alloy to 260 GPa: Implicationsfor composition of the core. J Geophysical Res 95:21737–21742.

McDonough WF, Sun S-S (1995) The composition of the Earth. Chem Geol 120(3-4):223–253. https://doi.org/10.1016/0009-2541(94)00140-4

Meier MMM, Bindi L, Heck PR, Neander AI, Spring NH, Riebe EI, Maden C, Baur H, Steinhardt PJ, Wieler W, Busemann H (2018) Cosmic history and a candidate parent asteroid for the quasicrystal-bearing meteorite Khatyrka. Earth Planet Sci Lett 490:122–131. https://doi.org/10.1016/j.epsl.2018.03.025

Miyahara M, El Goresy A, Ohtani E, Kimura M, Ozawa S, Nagase T, Nishijima M (2009) Fractional crystallization of olivine melt inclusion in shock-induced chondritic melt vein. Phys Earth Planet Inter 177(3-4):116–121. https://doi.org/10.1016/j.pepi.2009.08.001

Miyahara M, El Goresy A, Ohtani E, Nagase T, Nishijima M, Vashaei Z, Ferroir T, Gillet P, Dubrovinsky L, Simionovici A (2008) Evidence for fractional crystallization of wadsleyite and ringwoodite from olivine melts in chondrules entrained in shock-melt veins. Proc Nat Acad Sci 105(25):8542–8547. https://doi.org/10.1073/pnas.0801518105

Ohtani E, Kimura Y, Kimura M, Takata T, Kondo T, Kubo T (2007) Formation of high-pressure minerals in shocked L6 chondrite Yamato 791384: constraints on shock conditions and parent body size. Earth Planet Sci Lett 227:505–515

Oppenheim J, Ma C, Hu J, Bindi L, Steinhardt PJ, Asimow PD (2017a) Shock synthesis of five-component icosahedral quasicrystals. Sci Rep 7(1):15629. https://doi.org/10.1038/s41598-017-15771-1

Oppenheim J, Ma C, Hu J, Bindi L, Steinhardt PJ, Asimow PD (2017b) Shock synthesis of decagonal quasicrystals. Sci Rep 7(1):15628. https://doi.org/10.1038/s41598-017-15229-4

Palme H, Wlotzka F (1976) A metal particle from a Ca, Al-rich inclusion from the meteorite Allende, and the condensation of refractory siderophile elements. Earth Planet Sci Lett 33(1):45–60. https://doi.org/10.1016/0012-821X(76)90156-4

Reed SJB (1964) Composition of the metallic phases in some stone and stony-iron meteorites. Nature 204(4956):374–375. https://doi.org/10.1038/204374a0

Rubie DC, Jacobson SA, Morbidelli A, O'Brien DP, Young ED, de Vries J, Nimmo F, Palme H, Frost DJ (2015) Accretion and differentiation of the terrestrial planets with implications for the compositions of early-formed Solar System bodies and accretion of water. Icarus 248:89–108. https://doi.org/10.1016/j.icarus.2014.10.015

Sadoc A, Itié JP, Polian A, Lefebvre S, Bessière M, Calvayrac Y (1994) X-ray absorption and diffraction spectroscopy of icosahedral Al-Cu-Fe quasicrystals under high pressure. Phil Mag 70(4):855–866. https://doi.org/10.1080/01418639408240256

Shechtman D, Blech I, Gratias D, Cahn J (1984) Metallic phase with long-range orientational order and no translational symmetry. Phys Rev Lett 53(20): 1951–1954. https://doi.org/10.1103/PhysRevLett.53.1951

Stagno V, Aulbach S (2021) Redox processes before, during and after Earth's accretion affecting the deep carbon cycle. In: AGU monographs in press

Stagno V, Bindi L, Park C, Tkachev S, Prakapenka VB, Mao H-K, Hemley RJ, Steinhardt PJ, Fei Y (2015) Quasicrystals at extreme conditions: the role of pressure in stabilizing icosahedral $Al_{63}Cu_{24}Fe_{13}$ at high temperature. Am Mineral 100(11-12):2412–2418. https://doi.org/10.2138/am-2015-5412

Stagno V, Bindi L, Shibazaki Y, Tange Y, Higo Y, Mao H-K, Steinhardt PJ, Fei Y (2014) Icosahedral AlCuFe quasicrystal at high pressure and temperature and its implications for the stability of icosahedrite. Sci Rep 4:5869

Stagno V, Bindi L, Steinhardt PJ, Fei Y (2017) Phase equilibria in the nominally $Al_{65}Cu_{23}Fe_{12}$ system at 3, 5 and 21 GPa: Implications for the quasicrystal-bearing Khatyrka meteorite. Phys Earth Planet Inter 271:47–56. https://doi.org/10.1016/j.pepi.2017.08.005

Steurer W, Deloudi S (2009) Crystallography of quasicrystals. In: Concepts, methods and structures. Springer, Berlin

Stöffler D, Hamann C, Metzler K (2018) Shock metamorphism of planetary silicate rocks and sediments: proposal for an updated classification system. Meteorit Planet Sci 53(1):5–49. https://doi.org/10.1111/maps.12912

Suttle MD, Twegar K, Nava J, Spiess R, Spratt J, Campanale F, Folco L (2019) A unique CO-like micrometeorite hosting an exotic Al-Cu-Fe-bearing assemblage – close affinities with the Khatyrka meteorite. Sci Rep 9(1):12426. https://doi.org/10.1038/s41598-019-48937-0

Takagi S, Kyono A, Mitani S, Sugano N, Nakamoto Y, Hirao N (2015) X-ray diffraction study of the icosahedral AlCuFe quasicrystal at megabar pressures. Mater Lett 161:13–16. https://doi.org/10.1016/j.matlet.2015.08.057

Tomioka N, Bindi L, Okuchi T, Miyahara M, Iitaka T, Li Z, Kawatsu T, Xie X, Purevjav N, Tani R, Kodama Y (2021) Poirierite: a novel metastable Mg_2SiO_4 polymorph in shocked meteorites. Commun Earth Environ 2(1):16. https://doi.org/10.1038/s43247-020-00090-7

Tomioka N, Miyahara M (2017) High-pressure minerals in shocked meteorites. Meteorit Planet Sci 52(9):2017–2039. https://doi.org/10.1111/maps.12902
Tommasini S, Bindi L, Petrelli M, Asimow PD, Steinhardt PJ (2021) Trace element conundrum of natural quasicrystals. ACS Earth Space Chem 5(3):676–689. https://doi.org/10.1021/acsearthspacechem.1c00004
Xie, Sharp TG (2007) Host rock solid-state transformation in a shock-induced melt vein of Tenham L6 chondrite. Earth Planet Sci Lett 254(3-4):433–445. https://doi.org/10.1016/j.epsl.2006.12.001

Publisher's Note

Springer Nature remains neutral with regard to jurisdictional claims in published maps and institutional affiliations.